2130

An Analysis for Simulating Reservoir Performance Under Pressure Maintenance by Gas and/or Water Injection

K. H. COATS
MEMBER AIME

THE U. OF TEXAS
AUSTIN, TEX.

ABSTRACT

This paper describes a generalized analysis for calculating three-phase, three-dimensional flow in reservoirs. The analysis handles pressure maintenance type problems where fluid compressibility effects are negligible. A separate analysis for depletion type problems is described in another paper.[1] The calculations consist of numerical, simultaneous solution of the three-flow equations using the iterative alternating direction technique of Douglas and Rachford.[2] The mathematical details are fully described in the Appendix.

The analysis is a computerized mathematical model that accounts for gravity, and capillary and viscous forces, and allows arbitrary reservoir heterogeneity, geometry, well locations and rates. A unique aspect of the analysis is the simultaneous solution of only as many difference equations in each grid block of the reservoir as there are mobile phases present. Thus, while the analysis handles three-phase flow, the efficiency of the calculations (in a typical problem where three phases actually coexist only in a minor portion of the reservoir) is four to eight times greater than that of an analysis solving three equations in every block. The program may be applied to two-phase flow problems and to one-, two- or three-dimensional flow problems with negligible loss in efficiency, compared to programs specifically written for these subcases.

This paper also describes several applications of the analysis which illustrate some effects of gravitational and capillary forces in waterflooding of a heterogeneous reservoir. Another application indicates the utility of the program in simulating the fillup stage of water injection into a reservoir containing an initial free gas phase.

Computer times and costs for the applications performed are given to indicate the current expense of three-dimensional, three-phase reservoir simulation.

Original manuscript received in Society of Petroleum Engineers office May 28, 1968. Revised manuscript received Oct. 2, 1968. Paper (SPE 2130) was presented at the SPE Rocky Mountain Regional Meeting held in Billings, Mont., June 5-7, 1968.

[1]References given at end of paper.

INTRODUCTION

Under pressure maintenance by water and/or gas injection, fluid compressibility effects are generally negligible in producing operations. Although gas compressibility may be appreciable, the maintenance of pressure results in negligible time variation of gas density. In addition, the spatial variation of gas density is usually small in relation to the gas density itself. Producing schemes of pattern or flank waterflood and/or crestal gas injection, therefore, may be simulated with an analysis which presumes fluid incompressibility.

The computing efficiency of a numerical model for simulating incompressible fluid flow is as much as 50 percent greater than that of a compressible flow model. Therefore, an analysis for numerically simulating three-dimensional flow of three incompressible, immiscible phases was developed and programmed.

THE MODEL

The equations describing three-phase, incompressible flow are the continuity equation and Darcy's law for each flowing phase. Combining these equations and introducing capillary pressures gives the three flow equations:

$$\nabla \cdot \frac{k\, k_{rw}}{\mu_w} \nabla \Phi_w + i_w = -\phi\, S'_w \frac{\partial \Phi_w}{\partial t} + \phi\, S'_w \frac{\partial \Phi_o}{\partial t}, \quad \ldots\ldots\ldots\ldots (1a)$$

$$\nabla \cdot \frac{k\, k_{ro}}{\mu_o} \nabla \Phi_o + i_o = \phi S'_w \frac{\partial \Phi_w}{\partial t} - \phi\, (S'_w - S'_g) \frac{\partial \Phi_o}{\partial t} + \phi S'_g \frac{\partial \Phi_g}{\partial t} \quad \ldots\ldots\ldots\ldots\ldots\ldots (1b)$$

$$\nabla \cdot \frac{k\,k_{rg}}{\mu_g} \nabla \Phi_g + i_g = - \phi S'_g \frac{\partial \Phi_o}{\partial t} + \phi\, S'_g \frac{\partial \Phi_g}{\partial t} \quad \ldots\ldots\ldots\ldots \text{(1c)}$$

This set of equations is similar to those given by Douglas *et al.*[3] in their treatment of two-dimensional flow of two incompressible phases. The Appendix includes a derivation of these equations. In this differential form, the term S'_w is dS_w/dP_{cwo} where water-oil capillary pressure P_{cwo} is treated as a single-valued function of water saturation S_w. Similarly, the term S'_g is dS_g/dP_{cgo} where gas-oil capillary pressure, is taken as a single-valued function of gas saturation. The i terms are source terms corresponding to fluid injection and/or production.

Relative permeabilities to water and gas are considered single-valued functions of water and gas saturations, respectively. Relative permeability to oil is evaluated as $k_{ro} \times k_{rH}$, where k_{rH} is a single-valued function of water saturation and k_{ro} is a single-valued function of $(S_o + S_{wc})$.

In regions of the reservoir where only one or two mobile phases are present, Eq. 1 reduces to one or two equations. The Appendix shows how this reduction can be used to lower the computing requirements of the model considerably.

The computing time required by the analysis per time step is proportional to the number of blocks. For the same number of blocks, a three-dimensional calculation requires about 40 percent more time than a two-dimensional run. Relative computing times for one-, two- and three-phase flow calculations are given in Table 2 of the Appendix. These rules and ratios allow extrapolation of the computing times reported for the applications described in this paper to more dimensions, phases and/or blocks.

APPLICATION 1: GRAVITY FORCES AND SATURATION DISPERSION

Recent articles[4,5] discuss calculation techniques which minimize or eliminate the numerical dispersion that usually accompanies the standard second-order differencing used in the model described here. In some practical cases, sharp fluid saturation fronts (on an areal basis) occur, and attention should be paid to the reduction of numerical dispersion. In many cases, however, the numerical dispersion is insignificant in relation to a physically real dispersion (on an areal basis) caused by dip-normal gravity forces. This is especially true in gas injection cases where the large gas-oil density difference often results in a pronounced override of the oil by the gas. This override is reflected in areal (depth-averaged) saturation distributions as a considerably "dispersed" or smeared flood front. The smaller oil-water density difference results in a less pronounced but often significant underrunning of oil by water. Again, the result is a smeared, depth-averaged saturation profile.

In cases where these dip-normal gravity forces cause a significant override or underrunning, the physically real solution is an areally dispersed saturation front, and the methods using standard second-order differencing are capable of giving accurate solutions without resorting to an uneconomical number of grid elements to reduce block size and numerical dispersion. Apart from these dip-normal gravity forces, adverse mobility ratio tends to give low frontal saturations and a strongly dispersed saturation profile behind the front.

Fig. 1 illustrates the gravity dispersion for the case of a waterflood. The model described in the Appendix was employed in simulating water injection into a vertical cross-section 1,000 ft long by 60 ft thick. Relative permeability and other data for this 100-md, horizontal, homogeneous section are listed in Table 1. Calculations were performed using grids of 20 × 5 (block size 50 ft × 12 ft) and 10 × 5 (block size 100 ft × 12 ft). A linear capillary pressure-saturation curve with a slope equivalent to a transition zone (20 percent water to 80 percent water) of 17.5 ft was used. Initial water saturation was 20 percent (connate) throughout the section.

The lower half of Fig. 1 shows saturation contours after 4 years of water injection. These contours reflect the underrunning of water caused by gravity. This underrunning is reflected as dispersion in the areal or depth-averaged water saturation profile shown in the upper half of the figure. Refinement of the 20 by 5 grid resulted in an insignificantly sharper profile than that shown by the solid line in the upper half of Fig. 1; i.e., the dispersion indicated by the solid line is physically real and reflects the underrunning caused by gravity forces. The dotted line was calculated using a 10 × 5 grid and shows the error caused by numerical dispersion. A quantitative measure of the gravity dispersion is

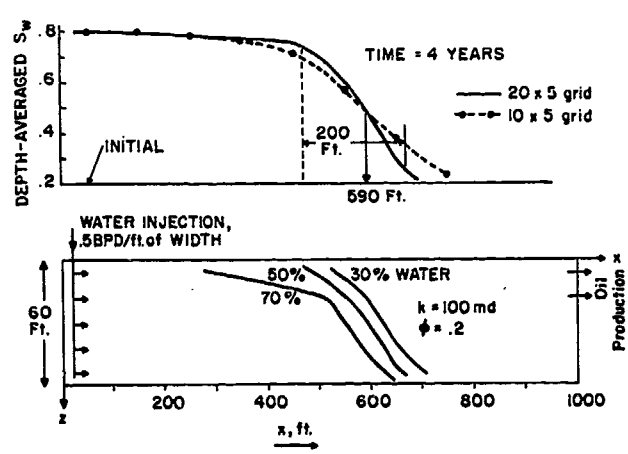

FIG. 1 — EFFECT OF GRAVITY ON A WATER-OIL DISPLACEMENT.

the ratio of the 200-ft transition zone* to the 590 ft traveled or a transition zone equal to 34 percent of the distance traveled.

An areal calculation for this reservoir that ignored gravity dispersion and achieved negligible numerical dispersion would yield a sharp saturation profile between 20 and 73 percent water, since the Buckley-Leverett[6] frontal saturation for the relative permeability curves of Table 1 is 73 percent. This result would be considerably in error in light of the 34-percent transition zone. Computing time on the UNIVAC 1108 for 4 years' injection into this 100-block cross-section was 40 seconds.

APPLICATION 2: EFFECT OF CAPILLARY FORCES

The effect of capillary pressure is generally negligible in two-dimensional areal calculations and assumption of zero capillary pressure is often justified in these cases. Two-dimensional, cross-sectional and three-dimensional calculated results for homogeneous reservoirs also are often insensitive to the level (within reason) of capillary forces. However, capillary forces are usually important in the case of heterogeneous, stratified reservoirs, a case frequently encountered in practice. If capillary pressure is assumed to be zero or the same for all layers, then calculated results will show injected water tending to "finger" through the most permeable layers of the reservoir.

*This transition zone is the distance between saturations of 74 percent and 26 percent that represents 0.9 and 0.1 normalized water saturation $\frac{(S_w - S_{wc})}{1 - S_{or} - S_{wc}}$.

TABLE 1 — FLUID AND RESERVOIR DATA FOR VERTICAL CROSS-SECTION

k = 100 md
ϕ = 0.2
Length L_x = 1,000 ft
Thickness h = 60 ft
Dip angle = 0
Specific gravity: water = 1
oil = .737
gas = .112
Viscosities: water = .6 cp
oil = 1.2
gas = .02
Initial water saturation .2 throughout
Initial oil saturation .8 throughout

			Saturation Tables				
S_w	P_{cwo}	k_{rw}	k_{rH}	S_{Liquid}	P_{cgo}	$\bar{k}_{ro}$	k_{rg}
.2000	2.000	.00000	.90000	.3500	2.000	.00000	.62000
.2500	1.875	.01000	.84500	.4000	1.846	.01200	.50000
.3000	1.750	.01800	.78000	.4500	1.692	.02900	.36000
.3500	1.625	.03000	.70000	.5000	1.538	.05000	.25000
.4000	1.500	.04200	.62000	.6000	1.231	.11200	.12000
.5000	1.250	.07500	.40000	.7000	.923	.21000	.05500
.6000	1.000	.12000	.17500	.8000	.615	.36000	.02300
.6500	.875	.14500	.10500	.9000	.308	.59000	.00800
.7000	.750	.17700	.05000	1.0000	.000	1.00000	-.00000
.7500	.625	.22200	.02000				
.8000	.500	.27000	-.00000				
.9000	.250	.45000	-.00000				
1.0000	.000	1.00000	-.00000				

.5 (B/D/ft of width) water injected at x = 0 over entire 60-ft thickness.
.5 (B/D/ft of width) production from top 40 percent of thickness at x = 1,000 ft.

If capillary pressure is included, the results may reverse entirely and show larger water saturations in the tighter layers. This is due to imbibition caused by the higher capillary forces in the lower permeability layers.

Two-dimensional calculations using the model described in the Appendix were performed for water injection into a heterogeneous, vertical cross-section. All data for the runs were identical to those given in Table 1 except for the stratification shown in Fig. 2. The total md-ft product was identical with the 100 x 60 figure of the former homogeneous case. The stratification consisted of layers ranging from 276 to 4 md in permeability.

The first run was performed with the same capillary-pressure curve (17.5-ft. transition zone) used for all layers. Calculated saturation contours after 4 years of injection are shown as the solid curves in Fig. 2. These contours show the more rapid advance of the 30 and 50 percent water-saturation contours in the high permeability layers 1, 3 and 5. The fingering is dampened considerably by crossflow (caused by gravity) into the tight layers 2 and 4. This effect of gravity is shown more clearly by the 70 percent water contour that shows the drainage of water from layer 1 to 3 caused by gravity forces acting over time.

A second run was performed using a different capillary-pressure curve for each layer. The slope of the curve was inversely proportional to the square root of permeability, in accordance with the Leverett J function.[7] Thus, the slope of the curve for the 276-md layer corresponded to a transition zone height of about 11.5 ft compared to 17.5 ft for the 100-md layer. The calculated saturation contours are shown by the dotted curves in Fig. 2. These curves show the opposite of the first run's results; that is, the contours are further advanced in the tighter layers. This effect is most pronounced for the 70-percent contour where the capillary forces have had more time to act. It is important to note that the high water saturations of the two tight layers is not due to x-direction flow from the injection well in those layers, but is caused almost entirely by crossflow under the action of capillary and gravity forces.

Fig. 3 shows the effect of J-function based capillary-pressure curves for each layer on the areal or depth-averaged saturation-vs-distance plot. The capillary forces promote crossflow into the

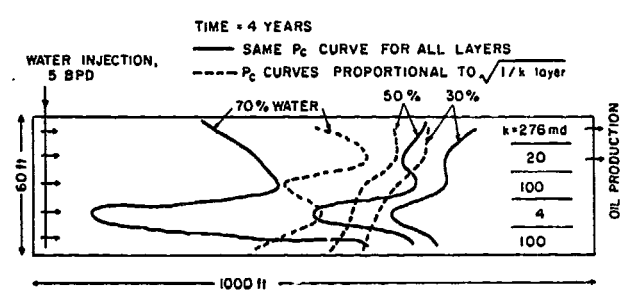

FIG. 2 — EFFECT OF CAPILLARY PRESSURE ON A WATER-OIL DISPLACEMENT.

tighter layers, thereby increasing vertical conformance. This is reflected by the sharper saturation profile shown by the dotted curve in Fig. 3.

These heterogeneous cross-section runs were performed using a 20 × 5 grid and required 54 seconds of 1108 time for 4 years of water injection.

APPLICATION 3: WATERFLOOD OF A RESERVOIR WITH AN INITIAL GAS SATURATION

An obvious application of a three-phase calculation is the estimation of waterflood performance for a reservoir containing an initial free-gas phase. To illustrate this application, a calculation was performed to simulate water injection into the vertical, homogeneous cross-section described in Table 1. A 20 × 5 grid was employed. Initial water saturation was connate (20 percent) in all layers and initial oil saturation was 80 percent in the bottom four layers, 65 percent in the top layer. Thus, initial gas saturation was 15 percent in the top layer or 3 percent on a depth-averaged basis. Water was injected at a rate of 0.5 BWPD/ft of width, and production of 0.5 BWPD was taken from the bottom layer at the right end of the section. No gas production could occur, therefore, until the gas accumulated in the top four layers and broke through into the bottom layer at the end of the section.

Fig. 4 shows calculated water- and gas-saturation profiles after 391 and 720 days of water injection. The profiles show that the gas is readily displaced by oil, and that it accumulates at the end due to production from the bottom layer only. Initial gas in place was 64 bbl; gas production was zero after 391 days and 7 bbl after 720 days. UNIVAC 1108 computer time for the 720-day run was 30 seconds.

APPLICATION 4: A FLANK WATERFLOOD

Fig. 5 shows an example reservoir 10,000 × 2,000 ft areally × 100 ft thick, dipping to the South at a constant angle of 11.5°. The areal heterogeneity consisted of a permeability gradation from 100 to 10 md from West to East as shown in the figure. The reservoir consisted of five layers of the following properties.

Layer	Permeability Factor	Porosity (percent)	Thickness (ft)
1	.1	10	15
2	1	18	10
3	4	20	25
4	.02	10	20
5	1.	16	30

The permeability of each layer at any areal point was the product of the above factor and the permeability for that areal point as shown in Fig. 5. (Relative permeability and fluid data are given in Table 1.) Water was injected into each of the three injection wells at a rate of 1,200 BWPD, and each of the four producing wells flowed 900 BWPD through a completion interval of layers 2 through 4. A three-dimensional grid of 20 × 10 × 5 was employed in the calculations.

Fig. 6 shows calculated water-saturation contours in the third (most permeable) layer after 600 days of water injection. The permeability gradation from West to East resulted in a higher ratio of viscous to gravity forces at the East than at the West side of the structure. These relatively greater viscous forces caused a slightly more pronounced spiking of water toward the production well at the East end. (See the 70-percent water contour.) Producing water-oil

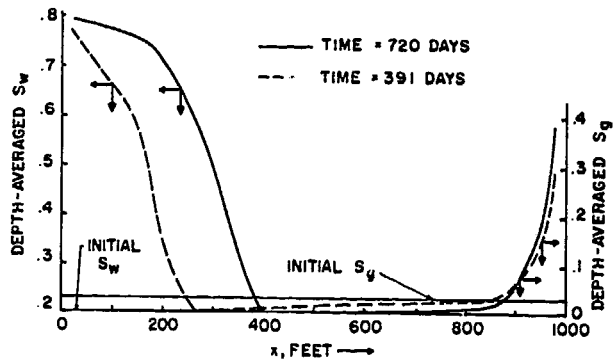

FIG. 4—CALCULATED WATER AND GAS SATURATION PROFILES, FILLUP STAGE OF A WATERFLOOD.

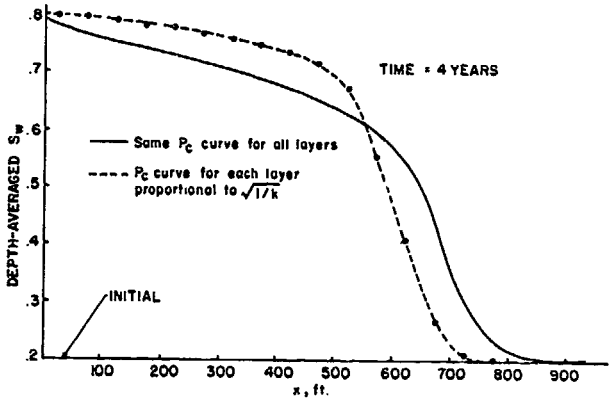

FIG. 3 — EFFECT OF CAPILLARY PRESSURE ON DEPTH-AVERAGED SATURATION PROFILE.

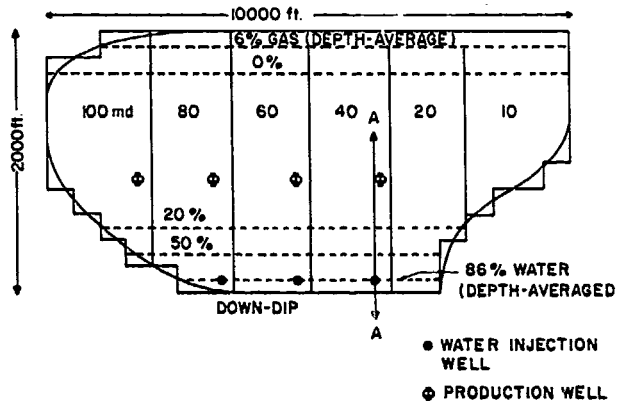

FIG. 5 — GEOMETRY AND INITIAL SATURATIONS FOR FLANK WATERFLOOD CALCULATION.

ratio at 600 days was 32 percent for the East well compared to 26 percent for the far-west well and 28 percent for the second well from the left.

Fig. 7 shows the fingering of water through the third layer. A single capillary-pressure curve was used for all layers. As previously discussed, if capillary curves inversely proportional to the square root of permeability were used, the fingering would be dampened considerably and vertical conformance would be considerably higher.

UNIVAC 1108 computing time for this 1,000-block, three-dimensional, 600-day run was 4 minutes.

COMPUTING AND TOTAL STUDY COSTS

Required UNIVAC 1108 computing times have been given for each of the four applications. A typical 1108 rental cost is $750/hour. The two-dimensional, two-phase, 100-block, 4-year simulation of Application 1 required about 40 seconds. This corresponds to a cost of (40/3,600) × $750 or $9. For larger reservoir (preserving the ratio of injection rate to gross reservoir size) and a 1,000-block, three-dimensional, two-phase flow calculation, the 40 seconds scales to

$$40 \times \frac{1{,}000 \text{ blocks}}{100 \text{ blocks}} \times 1.4 \frac{3\text{-D}}{2\text{-D}} = 560 \text{ seconds.}$$

Thus, this 1,000-block, three-dimensional calculation would cost about $125. If the computer program actually solved three simultaneous equations in every block, regardless of the number of mobile phases present, this cost would be about three times greater, or $350. (See Table 2 of the Appendix.)

The 1,000-block, three-dimension, 600-day calculation of Application 4 required 4 minutes. Therefore, a simulation covering 6,000 days for the same system would require about 40 minutes, or $500. If the program solved three equations rather than the necessary two in each block, the cost would be closer to $1,500.

An actual reservoir study employing simulation models involves man-time costs as well as computing-time costs. The ratio of these two varies widely depending upon the nature of the study. The gathering, interpretation and preparation of reservoir description and fluid property data for computer input can easily require 3 months for a three-dimensional study. At $30,000 per year this represents a cost of $7,500. If only a single case or a three-dimensional run were to be performed, then this cost might be five times the computing costs. If, however, a large number of cases were run to investigate different operational schemes and/or sensitivity of results to reservoir description data, then the computing cost might be five times the man-time cost.

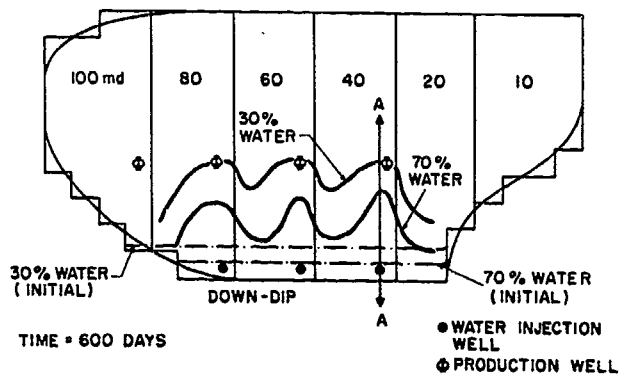

FIG. 6 — CALCULATED SATURATION CONTOURS IN THIRD LAYER.

CONCLUSIONS

A method is described for simultaneous, numerical solution of the three equations describing three-dimensional flow of three immiscible, incompressible phases in reservoirs. The model accounts for capillary, gravity and viscous forces and for arbitrary reservoir heterogeneity and geometry. The model is applicable to reservoirs produced under pressure-maintenance schemes of gas and/or water injection.

The solution method described entails simultaneous solution of only as many equations in any given block as there are mobile phases present. This achieves considerable savings in computing expense relative to a calculation which simultaneously solves three equations in all blocks. These savings result from the fact that relative computing times to simultaneously solve three, two and one equations are about 10:3:1.

Example applications illustrate (a) the tendency of dip-normal gravity forces to produce areally disperse flood fronts, and (b) the effect of capillary forces on waterflood performance in significantly stratified reservoirs.

NOMENCLATURE

$(A_{xm})_{i-\frac{1}{2},j,k}$ = x-direction transmissibility, for phase m, for flow between blocks i, j, k and $i-1, j, k$

$$= \left(\frac{k\, k_{rm}}{\mu_m}\right)_{i-\frac{1}{2},j,k} \frac{\Delta x}{\Delta y\, \Delta z}, \frac{.00633}{5.6146}$$

where k is in md, μ in cp

Z = elevation measured positive vertically downward, ft

k = permeability, md

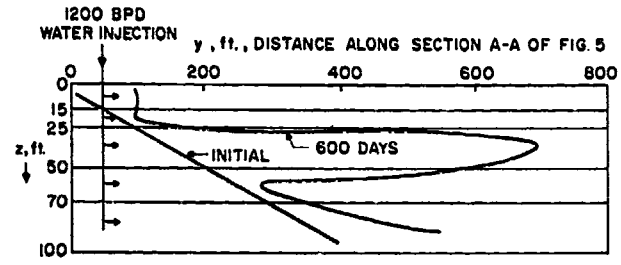

FIG. 7 — CALCULATED 70 PERCENT WATER CONTOURS IN SECTION A-A OF RESERVOIR UNDER FLANK WATERFLOOD.

k_r = relative permeability
k_{rH} = hydrocarbon relative permeability
k_{ro} = partial oil relative permeability
p = pressure, psia
P_{cgo} = gas-oil capillary pressure, $p_g - p_o$
P_{cwo} = water-oil capillary pressure, $p_o - p_w$
i = source term, volume of injected fluid/volume of reservoir/unit time
i_t = source term, B/D of injected fluid for an entire grid block
S = fluid saturation
S_{wc} = connate water saturation
S'_w = dS_w/dP_{cwo}
S'_g = dS_g/dP_{cgo}
t = time, days
Δt = time increment, days
u = superficial velocity
V_p = pore volume of grid block, bbl
ϕ = porosity
Φ = potential, $p - \gamma Z$
γ = specific weight, $\rho g/144\, g_c$ psi/ft
ρ = density, $\#_m$/cu ft
μ = viscosity, cp

SUBSCRIPTS

w or 1 = water
o or 2 = oil
g or 3 = gas

ACKNOWLEDGMENT

The author gratefully acknowledges the financial support covering his released time spent on this work. This work is a research project at The U. of Texas sponsored by Continental Oil Co., Shell Development Co. and the Sinclair Oil & Gas Co.

REFERENCES

1. Coats, K. H.: "A Mathematical Model for Simulating Three-Dimensional Three-Phase Fluid Flow in Reservoirs", The U. of Texas, Austin (Nov., 1968).
2. Douglas, Jim, Jr. and Rachford, H. H., Jr.: "On the Numerical Solution of Heat Conduction Problem in Two and Three Space Variables", *Trans.*, AMS (1956) Vol. 82, 421.
3. Douglas, Jim, Jr., Peaceman, D. W. and Rachford, H. H., Jr.: "A Method for Calculating Multi-Dimensional Immiscible Displacement", *Trans.*, AIME (1959) Vol. 216, 297-308.
4. Cavendish, J. C., Price, H. S. and Varga, R. S.: "Variational Methods for the Numerical Solution of Boundary Value Problems", Paper SPE 2034 presented at the SPE Numerical Simulation Symposium, Dallas (April 22-23, 1968).
5. Roper, W. A., Merchant, J. E. and Duval, C. A.: "Combination of Numerical and Analytical Techniques to Improve Waterflood Model Efficiency", SPE paper 2031 presented at SPE Symposium on Numerical Simulation of Reservoir Performance, Dallas (April 22-23, 1968).
6. Buckley, S. E. and Leverett, M. C.: "Mechanism of Fluid Displacement in Sands", *Trans.*, AIME (1942) Vol. 146, 107-116.
7. Leverett, M. C.: "Capillary Behavior in Porous Solids", *Trans.*, AIME (1941) 152-169.
8. Richtmyer, R. D.: *Difference Methods for Initial-Value Problems*, Interscience, Inc., New York (1957) 103.
9. Peaceman, D. W. and Rachford, H. H., Jr.: *J. Ind. Appl. Math.* (1955) Vol. 3, 28.
10. Coats, K. H., Nielsen, R. L., Terhune, M. H. and Weber, A. G.: "Simulation of Three-Dimensional, Two-Phase Flow in Oil and Gas Reservoirs", *Soc. Pet. Eng. J.* (Dec., 1967) 377-388.

APPENDIX

DERIVATION AND SOLUTION OF MATHEMATICAL MODEL FOR THREE-DIMENSIONAL FLOW OF THREE INCOMPRESSIBLE, IMMISCIBLE PHASES IN POROUS MEDIA

This analysis is a set of three partial differential equations, with each equation expressing conservation of mass for one of the flowing phases. The continuity equation

$$- \nabla \cdot (\rho_m \vec{u}_m) + \rho_m i_m = \phi \frac{\partial (\rho_m S_m)}{\partial t} \quad \ldots\ldots\ldots \text{(A-1)}$$

expresses the mass conservation for each flowing phase m, with m equaling 1, 2 and 3 corresponding to water, oil and gas, respectively. Darcy's law for each incompressible phase relates velocity to potential gradient as

$$\vec{u}_m = - k \frac{k_{rm}}{\mu_m} \nabla \Phi_m \quad \ldots\ldots\ldots \text{(A-2)}$$

where potential Φ_m is $p_m - \gamma_m Z$ and elevation Z is measured positive vertically downward. Cancellation of the constant density ρ_m from Eq. A-1 and combination of the two equations gives

$$\nabla \cdot (k \frac{k_{rm}}{\mu_m} \nabla \Phi_m) + i_m = \phi \frac{\partial S_m}{\partial t} \quad \ldots\ldots\ldots\ldots\ldots\ldots \text{(A-3)}$$

Additional relationships are the capillary pressure definitions,

$$P_{cwo}(S_1) \equiv p_2 - p_1 = \Phi_2 - \Phi_1 + (\gamma_1 - \gamma_2) Z \quad \ldots\ldots \text{(A-4)}$$

$$P_{cgo}(S_3) = p_3 - p_2 = \Phi_3 - \Phi_2 + (\gamma_2 - \gamma_3) Z \quad \ldots\ldots \text{(A-5)}$$

where water-oil capillary pressure and gas-oil capillary pressure are given functions of water and gas saturations, respectively. Finally, the sum of the saturations must equal 1:

$$S_1 + S_2 + S_3 = 1 \quad \ldots . \text{(A-6)}$$

Eqs. A-3 through A-6 are six equations in the six unknowns (Φ_m, S_m), $m = 1, 2, 3$.

The finite-difference representation of Eq. A-3 using standard second-order difference approximations is

$$\Delta A_m \, \Delta \Phi_m + i_{tm} = \frac{V_p}{\Delta t} \, \Delta_t S_m$$

where

$$\Delta A_m \, \Delta \Phi_m \equiv \Delta_x A_{xm} \Delta_x \Phi_m + \Delta_y A_{ym} \Delta_y \Phi_m + \Delta_z A_{zm} \Delta_z \Phi_m$$

$$\Delta_x A_{xm} \Delta_x \Phi_m \equiv (A_{xm})_{i+\frac{1}{2},j,k} (\Phi_{mi+1,j,k} - \Phi_{mi,j,k}) - (A_{xm})_{i-\frac{1}{2},j,k} (\Phi_{mi,j,k} - \Phi_{mi-1,j,k})$$

$$\Delta_t S_m = S_{m\,n+1} - S_{m\,n} \ldots . \text{(A-8)}$$

The subscripts i, j and k denote spatial position ($x = i\Delta y$, $z = k\Delta z$), and subscript n denotes time ($t = n\Delta t$).

The finite saturation change $\Delta_t S_m$ can be expressed in terms of potentials by using Eqs. A-4 and A-5:

$$\Delta_t S_1 = S_1' \Delta_t P_{cwo} = S_1' [\Delta_t \Phi_2 - \Delta_t \Phi_1]$$

$$\Delta_t S_3 = S_3' \Delta_t P_{cgo} = S_3' [\Delta_t \Phi_3 - \Delta_t \Phi_2]$$

$$\Delta_t S_2 = -\Delta_t S_1 - \Delta_t S_3 = S_1' \Delta_t \Phi_1 - (S_1' - S_3') \Delta_t \Phi_2 - S_3' \Delta_t \Phi_3$$

$$\ldots . \text{(A-9)}$$

In order that these $\Delta_t S$ terms may satisfy their definitions (Eq. A-8) exactly,

$$S_1' \equiv \frac{S_{1\,n+1} - S_{1\,n}}{(P_{cwo})_{n+1} - (P_{cwo})_n}$$

$$S_3' = \frac{S_{3\,n+1} - S_{3\,n}}{(P_{cgo})_{n+1} - (P_{cgo})_n} \quad \text{(A-10)}$$

That is, the S' terms are chords, not slopes, of the capillary pressure curves.

Substituting from Eq. A-9 into Eq. A-7 gives

$$\Delta A_m \, \Delta \Phi_m + i_{tm} = \sum_{\ell=1}^{3} C_{m\ell} \Delta_t \Phi_\ell \quad m = 1,2,3$$

$$\ldots . \text{(A-11)}$$

which are three equations in the three unknowns Φ_1, Φ_2 and Φ_3. The matrix of coefficients $\{C_{m\ell}\}$ is given by

$$C_{11} = C_1 \quad C_{12} = -C_1 \quad C_{13} = 0$$

$$C_{21} = -C_1 \quad C_{22} = C_1 + C_2 \quad C_{23} = -C_2$$

$$C_{31} = 0 \quad C_{32} = -C_2 \quad C_{33} = C_2 \, ,$$

$$\ldots . \text{(A-12)}$$

where $C_1 = -V_p \, S_1'/\Delta t$ and $C_2 = V_p \, S_3'/\Delta t$. These two latter terms are always positive.

Eq. A-11 is the mathematical model for incompressible, three-phase, three-dimensional flow in a porous medium.

The simultaneous solution of the three equations (Eq. A-11) is most efficiently described using matrix notation. Writing out the three equations in Eq. A-11, we obtain

$$\Delta_x A_{x1} \Delta_x \Phi_1 + \Delta_y A_{y1} \Delta_y \Phi_1 + \Delta_z A_{z1} \Delta_z \Phi_1 + i_{t1} = C_{11} \Delta_t \Phi_1 + C_{12} \Delta_t \Phi_2 + C_{13} \Delta_t \Phi_3$$

$$\Delta_x A_{x2} \Delta_x \Phi_2 + \Delta_y A_{y2} \Delta_y \Phi_2 + \Delta_z A_{z2} \Delta_z \Phi_2 + i_{t2} = C_{21} \Delta_t \Phi_1 + C_{22} \Delta_t \Phi_2 + C_{23} \Delta_t \Phi_3$$

$$\Delta_x A_{x3} \Delta_x \Phi_3 + \Delta_y A_{y3} \Delta_y \Phi_3 + \Delta_z A_{z3} \Delta_z \Phi_3 + i_{t3} = C_{31} \Delta_t \Phi_1 + C_{32} \Delta_t \Phi_2 + C_{33} \Delta_t \Phi_3 \ldots . \text{(A-13)}$$

We now define matrices and column vectors:

$$C \equiv \begin{pmatrix} C_{11} & C_{12} & C_{13} \\ C_{21} & C_{22} & C_{23} \\ C_{31} & C_{32} & C_{33} \end{pmatrix} \quad \underline{\Phi} = \begin{pmatrix} \Phi_1 \\ \Phi_2 \\ \Phi_3 \end{pmatrix}$$

$$AX = \begin{pmatrix} A_{x1} & 0 & 0 \\ 0 & A_{x2} & 0 \\ 0 & 0 & A_{x3} \end{pmatrix} \quad \underline{Q} = \begin{pmatrix} i_{t1} \\ i_{t2} \\ i_{t3} \end{pmatrix}$$

, ... (A-14)

and *AY*, *AZ* matrices are defined similarly to *AX*. By definition of matrix multiplication, the right side of Eq. A-13 is identically $C\Delta_t \underline{\Phi}$ where

$$\Delta_t \underline{\Phi} = \begin{pmatrix} \Delta_t \Phi_1 \\ \Delta_t \Phi_2 \\ \Delta_t \Phi_3 \end{pmatrix}$$

Similarly the left side is

$$\Delta_x AX \Delta_x \underline{\Phi} + \Delta_y AY \Delta_y \underline{\Phi} + \Delta_z AZ \Delta_z \underline{\Phi}$$

which we will condense to $\Delta A \Delta \underline{\Phi}$. We will preserve the definition

$$\Delta_x AX \Delta_x \underline{\Phi} = AX_{i+\frac{1}{2},j,k} (\underline{\Phi}_{i+1,j,k} - \underline{\Phi}_{i,j,k}) - AX_{i-\frac{1}{2},j,k} (\underline{\Phi}_{i,j,k} - \underline{\Phi}_{i-1,j,k})$$

and

$$AX_{i+\frac{1}{2},j,k} = \begin{pmatrix} (A_{x1})_{i+\frac{1}{2},j,k} & 0 & 0 \\ 0 & (A_{x2})_{i+\frac{1}{2},j,k} & 0 \\ 0 & 0 & (A_{x3})_{i+\frac{1}{2},j,k} \end{pmatrix}$$

Thus, Eq. A-13 can be simply written as

$$\Delta A \Delta \underline{\Phi} + \underline{Q} = C \Delta_t \underline{\Phi} \quad . . . . (A-15)$$

Eq. A-15 is a general form that describes one-, two- or three-phase incompressible flow in one, two or three dimensions. For one- or two-phase flow there is a change only in the dimension of the matrices and column vectors; there is no change in notation. For one- or two-dimensional flow, matrices *AZ* and/or *AY* are simply zero and, again, there is no change in notation. While subscripts are suppressed on Eq. A-15, it is understood that this equation applies at each spatial point (*i*, *j*, *k*) of the three-dimensional grid. For example, $\underline{Q}$ is actually $\underline{Q}_{i,j,k}$, etc. Therefore, for a 1,000-block, three-dimensional grid, Eq. A-15 represents 1,000 matrix equations or 3,000 scalar equations.

The solution of Eq. A 15 is obtained by using the Douglas-Rachford alternating direction procedure.[2] The equation is expressed implicitly in the respect that $\underline{\Phi}$ in the flow term $\Delta A \Delta \underline{\Phi}$ is taken at the new time level $n + 1$. All transmissibilities $(A_{x1})_{i+\frac{1}{2}}$, etc., are evaluated with relative permeabilities corresponding to the old (known) saturation distributions at time level *n*. The Douglas-Rachford procedure applied to Eq. A-15 gives the three-step calculation

$$\Delta_x AX \Delta_x \underline{\Phi}^* + \Delta_y AY \Delta_y \underline{\Phi}^k + \Delta_z AZ \Delta_z \underline{\Phi}^k + \underline{Q} = C (\underline{\Phi}^* - \underline{\Phi}_n) + H_k (\underline{\Phi}^* - \underline{\Phi}^k) ,$$

. . . . . (A-16a)

$$\Delta_x AX \Delta_x \underline{\Phi}^* + \Delta_y AY \Delta_y \underline{\Phi}^{**} + \Delta_z AZ \Delta_z \underline{\Phi}^k + \underline{Q} = C (\underline{\Phi}^{**} - \underline{\Phi}_n) + H_k (\underline{\Phi}^{**} - \underline{\Phi}^k),$$

. . . . . (A-16b)

$$\Delta_x AX \Delta_x \underline{\Phi}^* + \Delta_y AY \Delta_y \underline{\Phi}^{**} + \Delta_z AZ \Delta_z \underline{\Phi}^{k+1} + \underline{Q} = C (\underline{\Phi}^{k+1} - \underline{\Phi}_n) + H_k (\underline{\Phi}^{k+1} - \underline{\Phi}^k)$$

. . . . . (A-16c)

The matrix H_k is

$$H_k = \begin{pmatrix} h_k \Sigma A_1 & 0 & 0 \\ 0 & h_k \Sigma A_2 & 0 \\ 0 & 0 & h_k \Sigma A_3 \end{pmatrix}$$

where h_k is iteration parameter and the ΣA terms are sums of the transmissibilities for flow through the six faces of the block. The terms $\underline{\Phi}^*$, $\underline{\Phi}^{**}$ are intermediate potential solutions.

Eqs. A-16a through A-16c can be easily modified to calculate the potential changes over an iteration rather than the potential itself, with a resulting minimization of effects of round-off error. Subtraction of $\Delta A \Delta \underline{\Phi}^k$ from both sides of Eq. A-16a gives

$$\Delta_x AX \Delta_x \underline{PX} - (C + H_k) \underline{PX} = - BX$$

. . . . . (A-17a)

Subtraction of Eq. A-16a from Eq. A-16b gives

$$\Delta_y \, AY \, \Delta_y \, \underline{PY} - (C + H_k) \, \underline{PY} = - \underline{BY} \, ,$$

. . . . . (A-17b)

while subtraction of Eq. A-16b from Eq. A-16c gives

$$\Delta_z \, AZ \, \Delta_z \, \underline{PZ} - (C + H_k) \, \underline{PZ} = - \underline{BZ} \, .$$

. . . . . (A-17c)

The terms introduced are defined as

$$\underline{PX} \equiv \underline{\Phi}^* - \underline{\Phi}^k \qquad \underline{PY} \equiv \underline{\Phi}^{**} - \underline{\Phi}^k$$

$$\underline{PZ} \equiv \underline{\Phi}^{k+1} - \underline{\Phi}^k$$

$$\underline{BX} \equiv \Delta A \, \Delta \, \underline{\Phi}^k + \underline{Q} - C \, (\underline{\Phi}^k - \underline{\Phi}_n)$$

$$\underline{BY} \equiv (C + H_k) \, \underline{PX}$$

$$\underline{BZ} \equiv (C + H_k) \, \underline{PY} \quad . . . . . \text{(A-18)}$$

The *residual* $\underline{BX}$ is simply the residual of the equation (Eq. A-15) that is being solved. That is, $\underline{BX} \to 0$ as $\underline{\Phi}^k \to \underline{\Phi}_{n+1}$ where $\underline{\Phi}_{n+1}$ is the solution sought.

Each of equations in Eq. A-17 is a single equation in a single unknown, $\underline{PX}$, $\underline{PY}$ and $\underline{PZ}$, respectively. The forms of the equations are identical, so only the solution of Eq. A-17a needs to be described. That equation applies at each grid point (i,j,k) in the three-dimensional grid, and in subscripted, expanded form appears as

$$AX_{i+\frac{1}{2},j,k} \, \underline{PX}_{i+1,j,k} - (AX_{i+\frac{1}{2},j,k} + AX_{i-\frac{1}{2},j,k} + C_{i,j,k} + (H_k)_{i,j,k}) \, \underline{PX}_{i,j,k} + AX_{i-\frac{1}{2},j,k} \, \underline{PX}_{i-1,j,k} = - \underline{BX}_{i,j,k} \quad . . . . . \text{(A-19)}$$

This set of equations, written for fixed j and k and for $i = 1,2, \ldots, N_x$, (where N_x is the number of points in the x-line) forms a tridiagonal system. Richtmyer[8] describes the solution of such a system of equations as follows. The recursion relationship*

$$\underline{PX}_{i-1} = E_i \, \underline{PX}_i + \underline{F}_i \, , \quad . . . . \text{(A-20)}$$

is substituted into Eq. A-19 to obtain

$$E_{i+1} = [AX_{i+\frac{1}{2}} + AX_{i-\frac{1}{2}} \, [I - E_{i-1}] + C_i + H_{ki}]^{-1} \, AX_{i+\frac{1}{2}} \, ,$$

. . . . . (A-21a)

$$\underline{F}_{i+1} = [AX_{i+\frac{1}{2}} + AX_{i-\frac{1}{2}} \, [I - E_{i-1}] + C_i + H_{ki}]^{-1} \, [\underline{BX}_i + AX_{i-\frac{1}{2}} \, \underline{F}_i] \, .$$

. . . . . (A-21b)

where the superscript (−1) denotes the inverse of the 3×3 matrix in the brackets and I is the identity matrix. E is a 3×3 matrix and $\underline{F}$ is a column vector. Eqs. A-21a and 22b give all E_i, $\underline{F}_i$ for $i = 2, 3, \ldots, N_x + 1$ provided "starting" values E_2 and F_2 are found. These starting values are obtained from the boundary condition employed. In this work, no-flow boundary conditions are used so that $AX_{\frac{1}{2}} = 0$. Eqs. A-21a and A-21b then directly give

$$E_2 = [AX_{1\frac{1}{2}} + C_1 + H_{k1}]^{-1} \, AX_{1\frac{1}{2}}$$

$$\underline{F}_2 = [AX_{1\frac{1}{2}} + C_1 + H_{k1}]^{-1} \, \underline{BX}_1$$

. . . . . (A-22)

After solving for E_i, $\underline{F}_i$ for $i = 2, 3, \ldots, N_x + 1$, from Eqs. A-21 and A-22, $\underline{PX}_{N_x}$ is calculated from Eq. A-20 as

$$\underline{PX}_{N_x} = \underline{F}_{N_x+1}$$

where $\underline{E}_{N_x+1}$ is zero from Eq. A-21 and the no-flow boundary condition giving $AX_{N_x+\frac{1}{2}} = 0$. All other values of $\underline{PX}_i$ along the x-line, $i = N_x - 1, N_x - 2, \ldots, 1$, are then calculated by successive application of Eq. A-20. This x-line calculation is performed for all j and k values to cover the entire grid.

This solution process then is repeated to obtain $\underline{PY}$ by y-line calculation from Eq. A-17b and again to obtain $\underline{PZ}$ by z-line calculations from Eq. A-17c. The new iterate $\underline{\Phi}^{k+1}$ then is obtained as $\underline{\Phi}^k + \underline{PZ}$ and one iteration has been completed. That is, solution of Eqs. A-17a through A-17c constitutes one iteration. These iterations are repeated in cycles.[9,10]

Any one or combination of several closure tolerances may be employed to test for convergence. As previously stated, the residual $\underline{BX}$ approaches zero as the iterates $\underline{\Phi}^k$ approach $\underline{\Phi}_{n+1}$ so that the sum over the grid of $|(BX_m)_{i,j,k}|$ for each phase m is one possible tolerance. This is one of the more severe tolerances of those mentioned here. Another possibility is the maximum over the grid of $|(BX_m)_{i,j,k}|$. The incremental material balance for phase m is simply the ratio of the arithmetic sum over the grid of $(BX_m)_{i,j,k}$ to the net injection $\sum_{i,j,k} (i_{tm})_{i,j,k}$ and is a less severe tolerance. The lesser severity follows from the fact that the arithmetic summation allows cancellation of errors due to signs. Finally, a tolerance might be placed on the maximum change in potential $|\Phi_m^k - \Phi_m^{k-1}|$ in the last iteration over the grid for each phase m. In this work, tolerances have been employed, either

*Subscripts j,k are suppressed from this point on since they are fixed for the purpose of the x-line (i) calculation.

singly or in combination in a variety of reservoir calculations. While exceptions occur, a good incremental material balance alone (e.g., .001) generally implies a good solution. That is, in the great majority of cases encountered, insignificant changes in the solution occurred by iterating past the point where a good incremental material balance was first attained. We believe that a generally satisfactory compromise between the more or less severe tolerances is to employ the incremental material balance as the closure tolerance but to monitor (print out) one or more of the severe tolerance checks.

Considerable savings in the computing effort required in solution of Eqs. A-17a through A-17c results if one takes advantage of the fact that, at any given time step, some blocks experience only two- or even one-phase flow. The computational effort of solving Eqs. A-17a through A-17c is almost wholly represented by the equations in Eq. A-21. The savings involved in two- or one-phase flow comes from the fact that the dimensions of the matrices E, AX, C, etc., in Eq. A-21 are 3×3 for three-phase flow but only 2×2 for two-phase and 1×1 for one-phase flow, respectively. To show the reduced arithmetic effort in Eq. A-21 associated with the lower dimensions on those matrices requires expansion of the equation into scalar form and involves considerable additional nomenclature and space. In the interest of brevity and clarity, this expansion is not included here, but the work associated with each case is reported instead.

The total arithmetic operations per point required for solution of Eq. A-21 for all elements $\{e_{rs}\}$ and $\{f_r\}$ of the E matrix and $\underline{F}$ vector is given in Table 2 for the cases of three-, two- and one-phase flow.

TABLE 2 — COMPUTATIONAL WORK PER GRID POINT ASSOCIATED WITH SOLUTION OF EQ. A-21 FOR ELEMENTS OF E AND $\underline{F}$

	One-Phase Flow	Two-Phase Flow	Three-Phase Flow
Additions	4	14	37
Multiplications	3	21	62
Divisions	2	1	1
Total	9	36	100

This work includes the formation of elements C_{rs} of the C matrix but excludes the work of forming the sums of the transmissibilities ΣA in the elements of the H_k matrix. On a basis of total operations, this table shows ratios of 10:3:1 relative computing time for three-, two- and one-phase flow.

The FORTRAN IV program performing the calculations outlined above includes an integer array which denotes the current status of each block in the three-dimensional grid. The correspondence between the integer value and the character of the block is: −2 (all water), −1 (water-oil), 0 (three-phase), 1 (gas-oil), 2 (all gas) and 3 (all oil). In the solution of Eq. A-17, the program tests the value of the integer at each block and branches to a routine which solves Eq. A-21 for the appropriate dimension of the matrices C, E, etc., involved.

***